Eng. & Tech. Journal, Vol. 28, No.17, 2010

Artificial Neural Network Control of the Synchronous Generator AVR with Unbalanced Load Operating Conditions

Fadhil A. Hassan*& Helen J. Jawad*

Received on: 17/1/2010
Accepted on: 5/8/2010

Abstract

This paper proposes the using of artificial neural networks (ANNs') to control the synchronous generator automatic voltage regulator (AVR), with unbalance load operating conditions. The neural network for control a nonlinear system is described and used to demonstrate the effectiveness of the neural network for control the drives with nonlinearities. In this study, performances of a simulated neural network AVR evaluated for a wide range of unbalanced loads operating conditions. The variance factors are calculated, as an indicator of optimum operation, and their values are compared for different feedback signals and various unbalanced operating conditions. The optimum control is introduced, which gives an average variance factor in ANN controller is about 1.105%, whereas the average variance factor in traditional PI controller is about 2.035%.

Keywords: Synchronous generator, automatic voltage regulator, unbalanced load, neural network controller.

السيطرة بأستخدام الشبكات العصبية الأصطناعية على منظم الجهد الأوتوماتيكي للمولد التزامني في ظروف التشغيل للأحمال الغير متوازنة

الخلاصة

يقدم هذا البحث كيفية أستخدام الشبكات العصبية الأصطناعية كمسيطر ذكي على منظم جهد الأخراج الأوتوماتيكي في المولد التزامني الثلاثي الأطوار في ظروف التشغيل مع الأحمال ثلاثية الأطوار الغير متزنة. أُستُخدِمت الشبكة العصبية الموصوفة للسيطرة على النظام اللاخطى للتدليل على فاعلية الشبكات العصبية مع السواقات اللاخطية. قُيِمَ في هذه الدراسة أداء نموذج المحاكاة لمسيطر الشبكة العصبية في منظم الجهد الأوتوماتيكي عند مدى واسع للأحمال الغير متزنة. تم حساب معامل التباين كمؤشر للتشغيل الأمثل وتمت مقارنة قيمهُ لمختلف أنواع التغذية العكسية ومختلف ظروف التشغيل للحمل الغير متزن. قُدمت طريقة السيطرة المثلى والتي كان فيها متوسط معامل التباين في المسيطر العصبي حوالي (1.105%)، في حين أن متوسط معامل التباين في وحدة التحكم التقليدية PI (التناسبية التكاملية) حوالي (2.035%).

1. Introduction

Synchronous generator excitation control is one of the most important measures to enhance power system stability and to guarantee the quality of electrical power it provides. The main control function of the excitation system is to regulate the generator terminal voltage which is accomplished by adjusting the field voltage with respect to the variation of the terminal voltage [1]. Synchronous generators are used almost exclusively in power systems

*Electrical & Electronic Engineering Department, University of Technology/Baghdad

as a source of electrical energy. The generator is supplied with real power from a prime mover, usually a turbine, whilst the excitation current is provide by the excitation system. The excitation voltage E_f is supplied from exciter and is controlled by the automatic voltage regulator (AVR). Its aim is to keep the terminal voltage V equal to the reference value V_{ref} [2]. Since then, artificial neural networks (ANNs) are rapidly gaining popularity among power system researches. ANNs are extremely useful in the area of learning control. Consequently, the traditional adaptive control design has taken a new turn with advent of ANNs. ANNs are capable of learning from off-line simulation data and can then be trained to reflect the behavior of the system under various operating conditions [3]. In this study a synchronous generator is simulated in an unbalanced system and its performances are evaluated from different points of view. It is shown that AVR performances are significantly affected by the voltage feedbacks and their optimized values are determined by precise analysis of the simulation results.

2. Modeling of synchronous machine

For modeling a Synchronous machine system, simple circuit of its electrical diagram as shown in Fig. (1) is considered. For modeling and simulation of synchronous machine system, the following steps to be made step by step;

Step 1: Represent Synchronous Machine Circuit diagram.

Step 2: Represent System Mathematical equations.

Step 3: Calculate the Transfer Function of overall system.

Step 4: Convert to model block.

Step 5: Simulate the model using neural network.

2.1 A Description of Synchronous Machine

The armature windings are designed for generation of balanced three phase voltages and are arranged to develop the same number of magnetic poles as the field winding that is on the rotor. The rotor is also equipped with one or more short circuited windings known as damper winding. The rotor is driven by prime mover at constant speed and its field circuit is excited by direct current flow. The excitation may be provided through slip rings and brushes by means of AC generators mounted on the same shaft as the rotor of the synchronous machine. Modern excitation system usually use AC generator with rotating rectifiers, are known as brushless excitation [4].

2.2 Mathematical modeling and simulation of synchronous machine

The mathematical description of the synchronous machine is the same as all types of AC machines, which have two main problems: first, is the complex 3-phase represented differential equations, and second, is the time varying mutual inductance between stator and rotor winding, through the dynamic response of the SG. Simply, the first problem can be solved by using axis transformation to transfer the 3-phase parameters and quantities (like: voltage, current, flux….) to 2-phase parameters, which called Park's transformation or, Park model of SG. In which all stator quantities are transferred from phase a, b and c into equivalent dq axis new variables. Equations (1 to 4) show the approximate Park's transformation by neglecting the zero sequence parameters: [5, 6]

$$P(\theta)=\frac{2}{3}\begin{bmatrix}\cos(\theta) & \cos(\theta-\frac{2\pi}{3}) & \cos(\theta+\frac{2\pi}{3})\\ \sin(\theta) & \sin(\theta-\frac{2\pi}{3}) & \sin(\theta+\frac{2\pi}{3})\end{bmatrix} \quad \ldots.(1)$$

So ,

$$\begin{bmatrix}V_q^s\\ V_d^s\end{bmatrix}=|P(\theta)|.\begin{bmatrix}V_a\\ V_b\\ V_c\end{bmatrix} \quad \ldots(2)$$

$$\begin{bmatrix}I_q^s\\ I_d^s\end{bmatrix}=|P(\theta)|.\begin{bmatrix}i_a\\ i_b\\ i_c\end{bmatrix} \quad \ldots(3)$$

$$\begin{bmatrix}\Psi_q^s\\ \Psi_d^s\end{bmatrix}=|P(\theta)|.\begin{bmatrix}\Psi_a\\ \Psi_b\\ \Psi i_c\end{bmatrix} \quad \ldots(4)$$

The time varying problem can be solved by using the synchronously rotating reference frame model, in which all stator variables associated with fictitious winding rotating with the rotor at synchronous speed [6]. The transformation equations are:

$$F(\theta_e)=\begin{bmatrix}\cos(\theta_e) & -sin(\theta_e)\\ sin(\theta_e) & cos(\theta_e)\end{bmatrix} \quad ..(5)$$

$$\begin{bmatrix}v_q^e\\ v_d^e\end{bmatrix}=|F(\theta_e)|.\begin{bmatrix}v_q^s\\ v_d^s\end{bmatrix} \quad \ldots(6)$$

Figure (2) shows the synchronous generator stator and rotor windings in the dq-axis model, it's obviously that the effect of the field winding appears only in the d-axis, whereas the effect of the damper winding is equivalent to the rotor cage winding of an induction motor, which appears in both dq-axis circuits.

Therefore, the synchronously rotating reference frame equivalent circuits of the SG in d^e-q^e axes can be shown in fig (3). Equations (7 to 18) show stator and rotor circuits equations in d^e-q^e axes:

■ ***stator equations:*** [5, 6]

$$V_{qs}^e=-I_{qs}R_s-\omega_e\Psi_{ds}-\frac{d\Psi_{qs}}{dt} \quad ..(7)$$

$$V_{ds}^e=-I_{ds}R_s+\omega_e\Psi_{qs}-\frac{d\Psi_{ds}}{dt} \quad ..(8)$$

■ ***rotor equations:*** [5, 6]

$$0=I_{qr}R_r-\frac{d\Psi_{qr}}{dt} \quad ...(9)$$

$$0=I_{dr}R_r-\frac{d\Psi_{dr}}{dt} \quad ...(10)$$

$$V_f=I_fR_f+\frac{d\Psi_f}{dt} \quad ...(11)$$

Where all rotor parameters are referred to stator circuit and the mutual and self inductance of air gap (main) flux linkage are identical to L_{qm} and L_{dm} rotor to stator reduction.

$$\Psi_{qs}=L_{ls}I_{qs}+L_{qm}(I_{qs}+I_{qr}) \quad ..(12)$$

$$\Psi_{ds}=L_{ls}I_{ds}+L_{dm}(I_{ds}+I_{dr}+I_f) \quad ..(13)$$

$$\Psi_f=L_{lf}I_f+L_{dm}(I_{ds}+I_{dr}+I_f) \quad ..(14)$$

$$\Psi_{qr}=L_{lr}I_{qr}+L_{qm}(I_{qs}+I_{qr}) \quad ..(15)$$

$$\Psi_{dr}=L_{lr}I_{dr}+L_{dm}(I_{ds}+I_{dr}+I_f) \quad ..(16)$$

■ ***The electromagnetic torque:*** [5, 6]

$$T_e=-\frac{3}{2}P_1(\Psi_{ds}I_{qs}-\Psi_{qs}I_{ds}) \quad ..(17)$$

■ ***The motion equation:*** [5, 6]

$$T_{shaft}-T_e=\frac{J}{P_1}\frac{d\omega_r}{dt} \quad ..(18)$$

2.3 The per Unit (P.U.) d-q Model

The P.U. d-q model requires base quantities only for the stator. Though the selection of base quantities the following set is widely accepted:

$V_b = V_n\sqrt{2}$ peak stator phase nominal voltage .

$I_b = I_n\sqrt{2}$ Peak stator phase nominal current.

$S_b = 3V_nI_n$ Nominal apparent power.

$w_b = w_r$ Rated electrical angular speed ($w_r = 2pf / P_1$)

Based on this restricted set, additional base variables are derived [5, 6]:

$T_{eb} = \frac{S_b.P_1}{w_b}$ - Base torque.

$\Psi_b = \frac{V_b}{w_b}$ - Base flux linkage.

$Z_b = \frac{V_b}{I_b} = \frac{V_n}{I_n}$ - Base impedance.

$L_b = \frac{Z_b}{w_b}$ - Base inductance.

Inductances and reactance are the same in P.U. values. Though in some instances time is also provided with a base quantity $t_b = 1/w_b$, the inertia is, consequently,

$$H_b = \frac{1}{2}J\left(\frac{w_b}{P_1}\right)^2.\frac{1}{S_b}$$

The P.U. variables and coefficient (inductances, reactance, and resistances) are generally denoted by lowercase letters. Consequently, the P.U. d-q model equations, extracted from equation (7) through equation (18), become:

$$\frac{d\Psi_{qs}}{dt} = \omega_b[-v_{qs}^e - i_{qs}R_s - \omega_e\Psi_{ds}]$$
$$\frac{d\Psi_{ds}}{dt} = \omega_b[-v_{ds}^e - i_{ds}R_s + \omega_e\Psi_{qs}]$$
$$\frac{d\Psi_{qr}}{dt} = \omega_b[i_{qr}R_r]$$
$$\frac{d\Psi_{dr}}{dt} = \omega_b[i_{dr}R_r]$$
$$\frac{d\Psi_f}{dt} = \omega_b[V_f - i_fR_f]$$
$$\Psi_{qs} = l_{ls}i_{qs} + l_{qm}(i_{qs} + i_{qr})$$
$$\Psi_{ds} = l_{ls}i_{ds} + l_{dm}(i_{ds} + i_{dr} + i_f)$$
$$\Psi_f - l_{lf}i_f + l_{dm}(i_{ds} + i_{dr} + i_f)$$
$$\Psi_{qr} = l_{lr}i_{qr} + l_{qm}(i_{qs} + i_{qr})$$
$$\Psi_{dr} = l_{lr}i_{dr} + l_{dm}(i_{ds} + i_{dr} + i_f)$$
$$t_e = -(\Psi_{ds}i_{qs} - \Psi_{qs}i_{ds})$$
$$t_{shaft} - t_e = 2H\frac{d\omega_r}{dt}$$

….(19)

With t_e equal to the P.U. torque, which it should be positive when opposite to the direction of motion (generator mode). The Park transformation (matrix) in P.U. variables basically retains its original form. Its usage is essential in making the transition between the real machine and d-q model voltages (in general).

2.4 The steady state via the dq-model

During steady state, the stator voltages and currents are sinusoidal, and the stator frequency w_1 is equal to rotor electrical speed $w_r = w_1 =$ constant [6]:

$$V_{A,B,C}(t) = V\sqrt{2}\cos\left[w_1 - (i-1)\frac{2p}{3}\right]$$
$$I_{A,B,C}(t) = I\sqrt{2}\cos\left[w_1 - j_1 - (i-1)\frac{2p}{3}\right]$$

..(20)

Using the park transformation with $q_{er} = w_1t + q_0$ the d–q voltages is obtained:

$$V_{do} = \frac{2}{3}[V_A(t)\cos(-\theta_e) + V_B\cos\left(-\theta_e + \frac{2\pi}{3}\right)... + V_C\cos\left(-\theta_e - \frac{2\pi}{3}\right)]$$

$$V_{q0}=\frac{2}{3}[V_A(t)\sin(-\theta_e)+V_B\sin\left(-\theta_e+\frac{2\pi}{3}\right)+V_C\sin\left(-\theta_e-\frac{2\pi}{3}\right)] \quad \text{.....(21)}$$

Making use of equation (20) in equation (21) yields the following:

$$\left.\begin{aligned} V_{d0} &= V\sqrt{2}\cos q_0 \\ V_{q0} &= -V\sqrt{2}\sin q_0 \end{aligned}\right\} \quad \text{....(22)}$$

In a similar way, we obtain the current I_{d0} and I_{q0}:

$$\left.\begin{aligned} I_{d0} &= I\sqrt{2}\cos(q_0+j_1) \\ I_{q0} &= -I\sqrt{2}\sin(q_0+j_1) \end{aligned}\right\} \quad \text{.....(23)}$$

Under steady state, the d-q model stator voltages and currents are DC quantities. Consequently, for steady state, we should consider $d/dt = 0$ in equation (19):

$$\begin{aligned} V_{d0} &= w_r\Psi_{q0} - I_{d0}r_s \\ \Psi_{q0} &= l_{sl}I_{q0} + l_{qm}I_{q0} \\ V_{q0} &= -w_r\Psi_{d0} - I_{q0}r_s \\ \Psi_{d0} &= l_{sl}I_{d0} + l_{dm}(I_{d0}+I_{f0}) \\ V_{f0} &= r_f I_{f0} \\ \Psi_{f0} &= l_{fl}I_{f0} + l_{dm}(I_{d0}+I_{f0}) \\ I_{D0} &= I_{Q0} = 0 \\ \Psi_{D0} &= l_{dm}(I_{d0}+I_{f0}); l_d = l_{dm}+l_{sl} \\ t_e &= -(\Psi_{d0}I_{q0} - \Psi_{q0}I_{d0}) \\ \Psi_{Q0} &= l_{qm}I_{q0}; l_q = l_{qm}+l_{sl} \end{aligned} \quad \text{.....(24)}$$

From the previous equations and using equations (7 to 18) in P.U form, with ignoring the effect of the damper winding (for simplicity), we can simulate the per-phase dynamic reference frame model of a synchronous generator as shown in fig.(4). In this research the per-phase model is not sufficient to perform the unbalance load operation of the S.G. Therefore, a three-phase model is required, which can be simply represented by simulate three of per-phase stator-rotor model with one torque-speed simulation block, as shown in fig. (5).

3. Traditional AVR system

An adaptive proportional-integral (PI) controller is the most powerful method to regulate terminal voltage of the S.G used with different operating loads and power factors [1]. The operating principle is to sense the terminal phase voltage and use it as a feedback signal through the PI controller to generate command setting signal which adapt the excited voltage of the S.G, which gives an acceptable behavior of the system for different balance loads. This controller can be easily adapted by using trial and error method to obtain the proportional gain (k_p) and the integral gain (k_i). the overall system is shown in fig. (5), and the output performance of the system at full-load operation shown in fig. (6), with k_p=1 k_i=2.35 and the feedback signal can be taken from any output phase (A,B or C).

Unfortunately, when the system operated with unbalanced load, as shown in fig. (7), a problem occurs from the confusion of: from which phase the feedback signal can be taken? The suitable operation criteria is depends on calculating the **variance factor** of the three phase output voltage with respect to the desired output voltage, where the smallest variance factor gives the best operation and best control. Table (1)

gives the variance factor of the output voltage when the feedback signal was taken from phase A, B and C for different unbalanced operating loads.

4. RMS and Mean feedback control

One of used method to overcome the effect of unbalance operation, is to calculate the root mean square (RMS) or the Mean value of the unbalance output three phase voltages, and used these values as a feedback signal to control the excitation voltage through the PI controller, instead of sensing one phase voltage. This system can be easily implemented by adding RMS or Mean calculation block to the previous simulation diagram as shown in figs. (8 & 9). Table 2 shows the variance factor of the RMS and Mean method for different unbalance loads.

5.1 Artificial Neural Networks

Nowadays, we have seen extensive researches and developments effort to use the intelligent system in many industrial applications, because of its strong features like: learning ability, massive parallelism, fast adaptation, inherent approximation capability, and high degree of tolerance [7]. Neural Network Controller (NNC) was effectively introduced to improve the performance of nonlinear system, which are a powerful tools used to predict the optimum performance for both identification and control system. The universal approximation capabilities of multi-layer perceptron make it popular choice for modeling nonlinear systems and for implementing general-purpose controllers. The neural network is an intelligent system which could be learned or trained using an actual existing input and output table, learning or training can be achieved in real-time or off-time operation [3, 7].

5.2 Design of Neural Network

These features give a good ability to solve the problem of unbalance load operation, by adapt a suitable neural network to predict the desired feedback signal from the three phase unbalanced voltages. Fig. (10) shows the structure of used neural network in this work is consist of **three input neurons** which are the synchronous generator output phase voltages (V_a, V_b, and V_c), and **one output neurons** which is the feedback signal. Also, consist of **five hidden layers**. The training process done by using large number of input and output data, obtained from different unbalance 3-phase load operation. The back-propagation Levenberg-Marquardt training algorithm is used, which design to approach second-order training speed.

Fig. (11) shows the MSR (mean square error) of the training process. The overall simulation with the neural network can be shown in fig. (12). Table 3 shows the variance factor for different unbalanced loads. Table (4) summarized the variance factor for different feedback methods at different unbalance operating load.

6. Conclusions

- From the results obtained it's obviously that the neural network feedback control gives smallest average variance factor of the output voltages, which is about 1.105%. Whereas, in the traditional PI controller and both RMS and Mean feedback methods the average variance factors are 1.707% and 2.035% respectively. That means the automatic voltage controller of the synchronous generator gives the best performance of the terminal voltage

with using the Neural Network Controller.

● The variance factors of symmetrical unbalanced load, such as (1_0.8_0.6) and (0.8_0.6_1), are not equals in the NNC link other methods, but it is still the best performance. An additional training data taking in account that cases and consisting different symmetrical unbalanced loads can be used to improve the NNC performance.

7. References

[1]Alireza Sedaghati. " *A PI Controller Based On Gain-Scheduling for Synchronous Generater*", Electrical Engineering, Vol.14,No.2,2006 .

[2]J.Machowski,J.W.Bialek and S.Robak, " *Excitation Control System for Use with Synchronous Generators*", IEE Proc. Gener. Transm. Distrib. , vol 145,No.5,September 1998.

[3]Salah G . Foda "*ANN Based Power System Stabilizers for large Synchronous Generators*", J.King Saud Univ., Vol . 14, Eng. Sci. (2),PP.199-209,2002.

[4]Tin Win Mon, and Myo Myint Aung, "*Simulation of Synchronous Machine in Stability Study for Power System*", ISSN 1307-6884 vol. 29 May 2008.

[5]Taylor and Francis Group, "*SynchronousGenerators*",Handbook,2006.

[6]Bimal K. Bose, " *Modern Power Electronic and AC Drives*", Prentice Hall, 2002.

[7]Howard Demuth, Mark Beale, "*Neural Network Toolbox*", Copyright 1992-2004 by the Math Work, Inc.

Table (1) Variance factor of direct feedback

Unbalance load P.U.			% variance factor Feedback from		
A	B	C	A	B	C
1	0.8	0.6	1.62	2.61	3.6
0.6	1	1	1.02	1.19	1.19
0.8	0.6	1	2.61	3.6	1.62
0.6	1	0.8	3.6	1.62	2.61
1	1	0.8	1.19	1.19	1.02
0.8	0.8	0.6	2.51	2.51	2.37

Table (2) Variance factor of RMS and Mean value feedback signal

Unbalance load P.U.			% variance factor Feedback method	
A	B	C	RMS	Mean
1	0.8	0.6	2.66	3.29
0.6	1	1	1.38	1.45
0.8	0.6	1	2.66	3.29
0.6	1	0.8	2.66	3.29
1	1	0.8	0.59	0.62
0.8	0.8	0.6	0.29	0.25

Table (3) Variance factor of neural network controller

Unbalance load P.U.			%variance factor Of NNC
A	B	C	
1	0.8	0.6	1.29
0.6	1	1	0.94
0.8	0.6	1	2.6
0.6	1	0.8	1.08
1	1	0.8	0.54
0.8	0.8	0.6	0.18

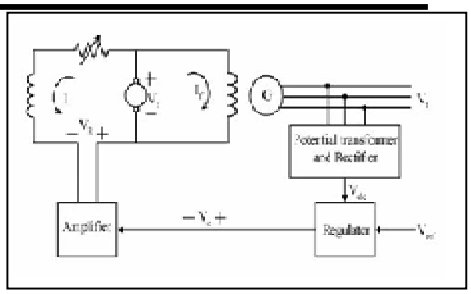

Figure (1) A close loop control of S.G. and its excitation system.

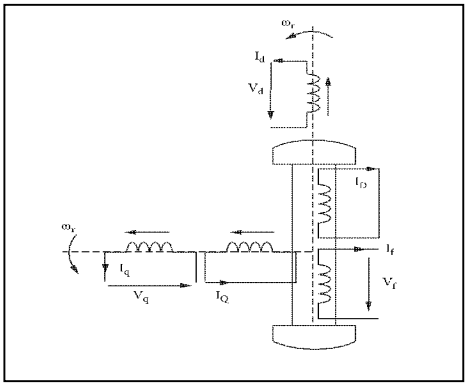

Figure (2) S.G. windings in qd-axis

Table (4) Variance factor of different feedback methods

Unbalance load P.U.			% Variance factor		
			Feedback from		
A	B	C	RMS	Mean	NNC
1	0.8	0.6	2.66	3.29	1.29
0.6	1	1	1.38	1.45	0.94
0.8	0.6	1	2.66	3.29	2.6
0.6	1	0.8	2.66	3.29	1.08
1	1	0.8	0.59	0.62	0.54
0.8	0.8	0.6	0.29	0.25	0.18
Average			1.707	2.035	1.105

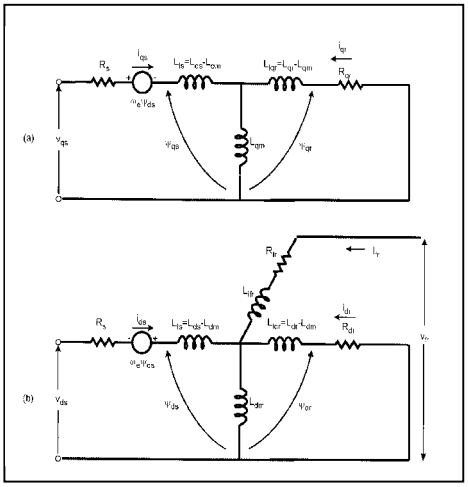

Figure (3) Stator and rotor equivalent circuits in qd-axis

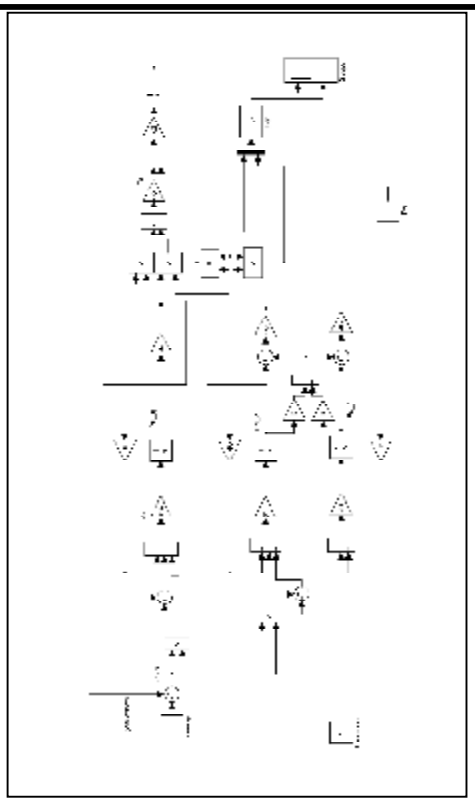

Figure (4) Simulation of per-phase S.G.

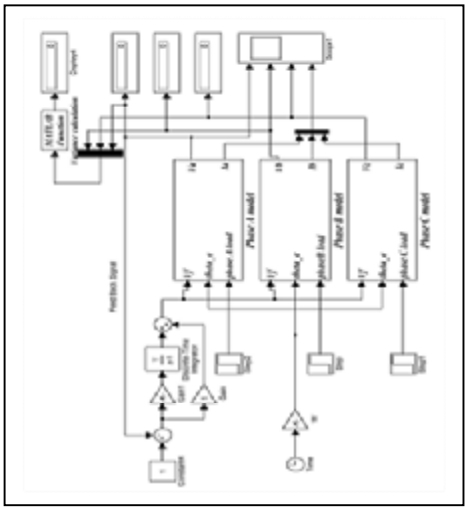

Figure (5) 3-phase simulation of S.G. with PI excitation controller

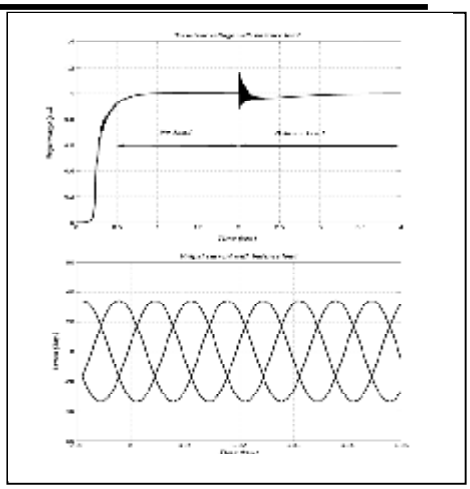

Figure (6) Terminal voltage and current with balanced load operation

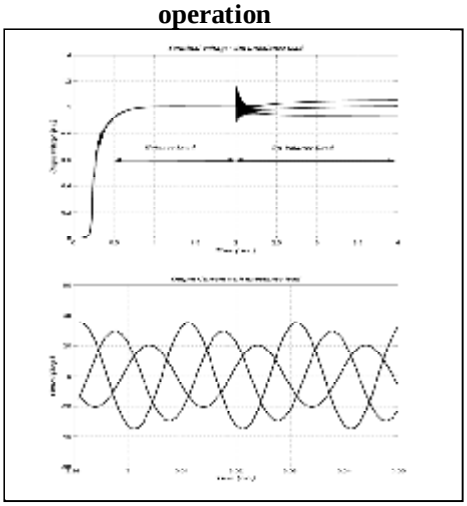

Figure (7) Terminal voltage and current with unbalanced load operation

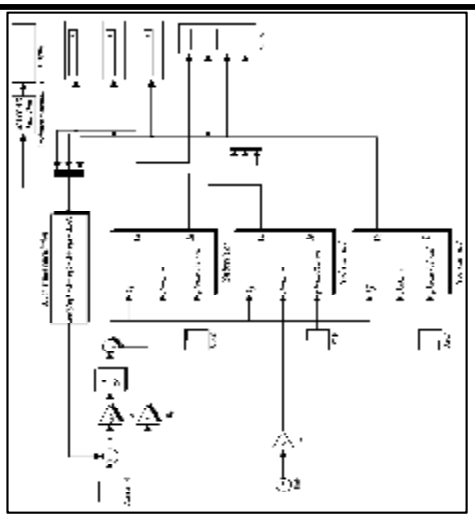

Figure (8) Excitation control with mean value feedback

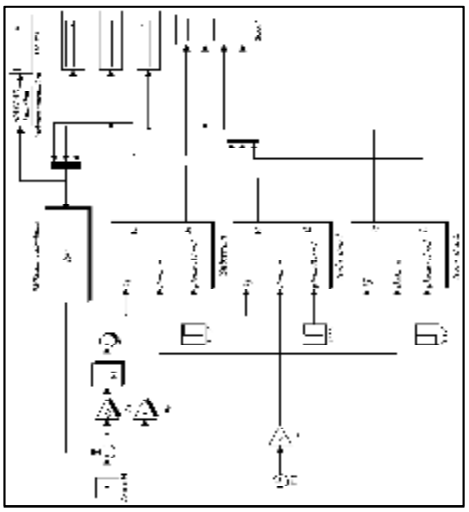

Figure (9) Excitation control with RMS value feedback

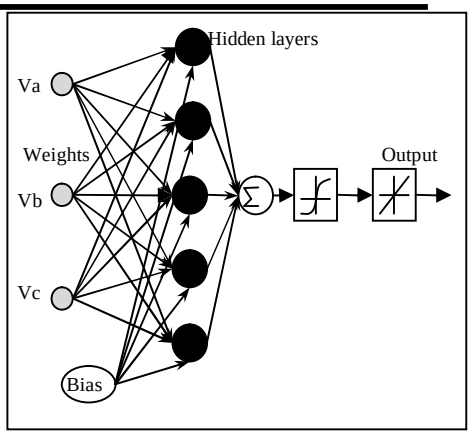

Figure (10) Neural Network structure

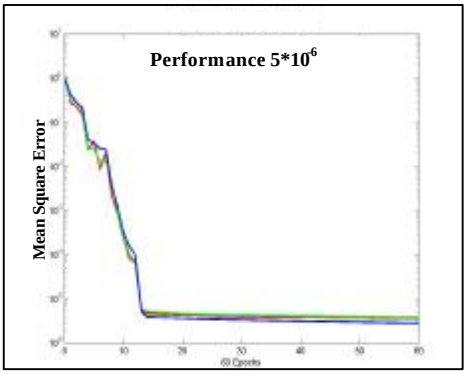

Figure (11) *Training MSE*

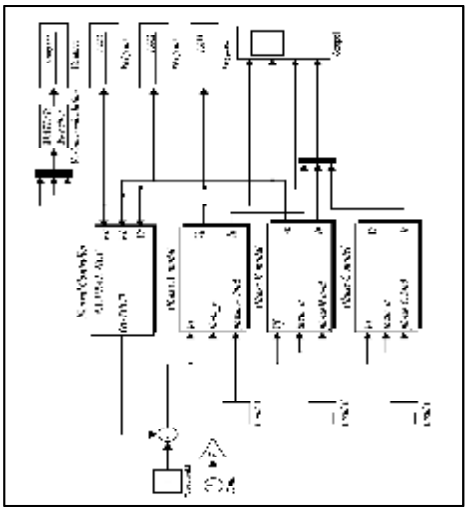

Figure (12) Excitation control with NNC